Journal of Offshore Structure and Technology
Research paper
Vol 11, issue 1,2024
Receiving date:18-5-2024
Acceptance- 21-05-2024
Publication 22-05-2024

Improved Marine Wind Farm Layout

Carlos Armenta-Déu
(cardeu@fis.ucm.es)
1Professor, Department of Matter Structure, Thermal Physics and Electronics, Faculty of Physical Sciences, Complutense University of Madrid, 28040 Madrid, Spain

ABSTRACT

This work proposes a new marine wind farm layout. The new configuration is based on the hybridization of alternating lift-force and drag-force wind turbines. Lift-force wind turbines are characterized by a high output power and large dimensions, while drag-force wind turbines have moderate power output and reduced size. The proposed layout inserts the drag-force turbines in the free space the lift-force turbines leave, using the turbulent wind to generate power and reduce the turbulence index in the leeward direction. This configuration shortens the distance between the lift-force wind turbines, increasing the power surface density of the wind farm. The new configuration improves the performance and generates extra energy due to the higher power density and the insertion of drag-force wind turbines. Wind farm global power increase depends on the drag-force turbine efficiency, the turbulence index reduction, and the lift-force turbine size. A simulation process, which runs on the above characteristics, results in a 20% global power increase for drag-force wind turbine standard characteristics operating in current conditions.

Keywords: Wind energy; Wind Marine Farm; Lift-force and drag-force wind turbines; Hybrid layout; Performance improvement; Output power increase; Turbulence index.

INTRODUCTION

The more and more use of open areas on the sea for marine wind turbine installation requires a more detailed study of how using these areas can be improved [1-3]. Marine wind farms benefit from laminar wind flow, regular wind speed regime, no interference by natural or artificial obstacles, and lack of human activities influence. These advantages favor the continuous increase of the wind turbine size. Now, reaching a nominal output power of 8 MW is expected to reach 20 MW in the future [4].

The size of the marine wind turbines forces to increase the distance between two adjacent turbines to avoid the negative influence of turbulence created by the turbine itself when the wind passes through them [5-6]; the increase in the distance limits the capacity of a marine wind farm to generate as much power as expected due to the size of the installed turbines.

Even if there is a large open area to install a marine wind farm, a better harnessing of this free space results in an improvement of the wind farm and an increase in the global output power. To this goal, different solutions arise: to improve the power-to-used surface ratio, say increase the surface power density, to install more efficient wind

Journal of Offshore Structure and Technology
Research paper
Vol 11, issue 1,2024
Receiving date:18-5-2024
Acceptance- 21-05-2024
Publication 22-05-2024

turbines, or to install additional wind turbines without penalizing the performance of the existing ones.

The use of more efficient wind turbines requires the advance of technological development in the components and structure of today's marine wind turbines, which means time to reach the goal [7-13]. The increase of the surface power density also requires the development of better technology that makes more efficient use of the wind resource, especially the turbulent flow; this implies a change in the design of the wind turbine blades [14-16]. Finally, the additional turbine installation with no interference effects with the existing ones requires the harnessing of turbulent wind flow, which is not compatible with the design and structure of current marine wind turbines [17-18].

A solution to this latter option would be using drag-force wind turbines, which operate with turbulent wind flows at moderate-high efficiency, also reducing the turbulence index in the leeward direction [19-20]. These turbines can be installed in the free space left by the giant wind turbines that operate under the lift-force mode, obtaining a double effect: the power generation of the installed drag-force wind turbines and the reduction of the turbulence index, which allows for reducing the distance between turbines, so increasing the power density of the marine wind farm.

THEORETICAL FOUNDATIONS

The current configuration of a wind farm requires a separation distance between two adjacent wind turbines of 8 to 10 times the diameter of the wind turbine rotor in the wind direction and 3 to 5 times in the sideway direction [21-23].

The required distance between adjacent wind turbines is due to the turbulent flow that generates drag-force effects on the rotor blades, reducing the lift force [24-26], thus, the torque and power generation, and creating stress and fatigue on the blade material which results in cumulative damage that may break the blade with time [27-28].

Wind dynamic force splits in the lift, drag, and pushing force; considering the last force tends to move the turbine to the leeward side, with no effects on the generated torque, wind lift-force and drag-force onto the rotor blade can be expressed as [22,23]:

$$F_L = \frac{\pi}{8} C_L \rho_{air} D^2 u^2$$
$$F_D = \frac{\pi}{8} C_D \rho_{air} D^2 u^2 \qquad (1)$$

F_L and F_D are the lift-force and drag-force, C_L and C_D are the lift-force and drag-force coefficients, ρ_{air} is the air density, D is the wind rotor diameter, and u is the wind speed.

Lift-force and drag-force coefficients define the corresponding dynamic wind force fraction; they depend on the wind direction regarding the rotor blade and the turbulent index through the Reynolds numbers (Figure 1) [29].

Journal of Offshore Structure and Technology
Research paper
Vol 11, issue 1,2024
Receiving date:18-5-2024
Acceptance- 21-05-2024
Publication 22-05-2024

In marine environments, wind tends to flow under a low turbulent regime with a Reynolds number below 106, which we may consider the threshold between low and high turbulent regimes [30]. In such conditions, according to the information shown in Figure 1, as the angle of attack increases, the drag-force coefficient rises with a lowering Reynolds number; this situation increases drag forces to the detriment of lift-force ones, which reduces power generation in conventional wind turbines but favors the energy production by drag-forcewind turbines.

The angle of attack in a drag-force wind turbine is modified by changing the pitch angle to the appropriate value to optimize the drag-to-lift-force coefficient ratio.

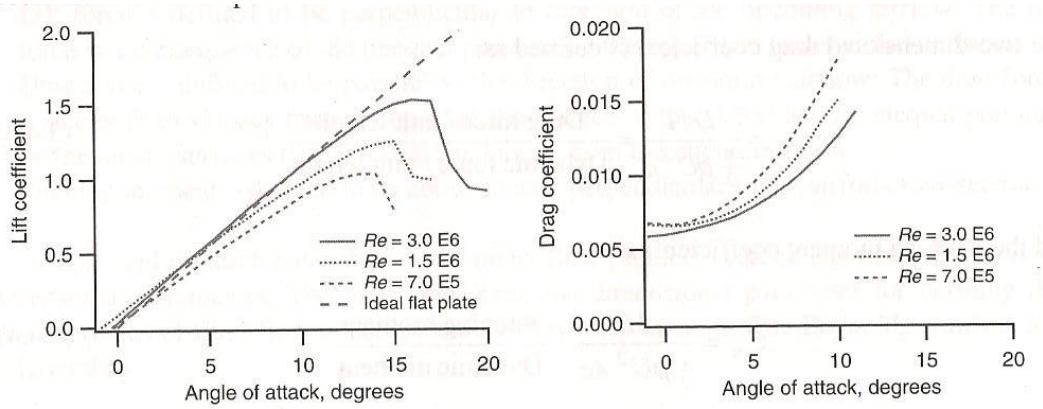

Figure 1 Lift-force and drag-force coefficient evolution with angle of attack and Reynolds number

In current conditions, the pitch angle is about 2º, a value that optimizes the performance of lift-force wind turbines [31]. Applying this value to Figure 1, we obtain a drag-to-lift-force coefficient ratio of:

$$C_r = C_D / C_L = 0.0064/0.23 = 0.028 \qquad (2)$$

If we reduce the angle of attack to a null value:

$$C_r = C_D / C_L = 0.007/0.03 = 2.23 \qquad (3)$$

Comparing values from equations 2 and 3, we realize that the drag-to-lift-force ratio increases by 80 times, which shows that the drag-forcebecomes the predominant one.

If we analyze the output power for a conventional high-quality marine wind turbine of 120 m diameter, operating under a lift-force or drag-force mode at a wind speed of 14 m/s, we obtain for the lift-force mode:

Journal of Offshore Structure and Technology
Research paper
Vol 11, issue 1,2024
Receiving date:18-5-2024
Acceptance- 21-05-2024
Publication 22-05-2024

$$P_t = \frac{\pi}{8} C_p \rho_{air} D^2 u^3 = \frac{\pi}{8}(0.4)(1.255)(120)^2(14)^3 = 7.79x10^6 W = 7.8MW \qquad (4)$$

Corresponding to a lift-force of:

$$F_L = \frac{\pi}{8}(0.23)(1.255)(120)^2(14)^2 = 319926N \approx 320kN \qquad (5)$$

Since the drag-forceis:

$$F_D = \frac{\pi}{8}(0.0064)(1.255)(120)^2(14)^2 = 8902N \approx 8.9kN \qquad (6)$$

The wind turbine output power operating under drag-forcemode is:

$$P_t = (7.8)(8.9/320) = 0.217MW \qquad (7)$$

This value is meaningless for a marine wind turbine, especially compared to the current output power of 7.8 MW.

For a null pitch angle, we have:

$$\begin{aligned} F_L &= \frac{\pi}{8}(0.03)(1.255)(120)^2(14)^2 = 41729N \approx 41.7kN \\ F_D &= \frac{\pi}{8}(0.007)(1.255)(120)^2(14)^2 = 9737N \approx 9.8kN \end{aligned} \qquad (8)$$

The results show that operating under this condition, null pitch angle, the lift-force continues being the predominant force, but we reduce the output power to 1 MW under lift-force mode, with a slight output power increase under drag-forcemode, from 0.217 MW to 0.239 MW, barely 10% increase; it is clear that this configuration is unsuitable.

Considering the above analysis, the solution for drag-force wind turbine insertion is to use specific drag-force wind turbines with modified blade shapes, which admit pitch angles higher than currently accepted for conventional turbines. Previous study shows that we can operate with drag-forcewind turbines under variable pitch for turbulent flows [29].

Developing a simulated analysis for a dag force wind turbine operating at a pitch angle of 15º, corresponding to a drag-force coefficient of 0.035, we obtain an equivalent output power of:

$$P_t = (7.8)(48.7/320) = 1.2MW \qquad (9)$$

Where the upper value of the fraction in equation 9 derives from:

$$F_D = \frac{\pi}{8}(0.035)(1.255)(120)^2(14)^2 = 48.7kN \qquad (10)$$

Journal of Offshore Structure and Technology
Research paper
Vol 11, issue 1,2024
Receiving date:18-5-2024
Acceptance- 21-05-2024
Publication 22-05-2024

The output power in equation 9 corresponds to a wind turbine of diameter:

$$D = \left(\frac{8P_t}{\pi \rho_{air} u^3} \right)^{1/2} = \left(\frac{8x1.2x10^6}{1.255\pi(14)^3} \right)^{1/2} = 47.1m \qquad (11)$$

Therefore, the drag-forcewind turbine has a rotor area of 16% of the conventional wind turbines and a 60% smaller diameter, which is compatible with the insertion process.

MARINE WIND FARM LAYOUT

Based on these premises, adopting the minimum distance between adjacent wind turbines to maximize the harnessing of the used area, and considering a rectangular cell of 8D length and 3D width (Figure 2), the surface power density of a marine wind farm results:

$$\sigma_P = \frac{P}{S} = 4\frac{(1/2)C_p \rho_{air} (\pi/4) D^2 u^3}{24D^2} = \frac{\pi}{48} C_p \rho u^3 \qquad (12)$$

Equation 12 shows that the surface power density of a marine wind farm depends on the wind turbine quality through the power coefficient, C_p, the air density, ρ_{air}, and wind speed, u.

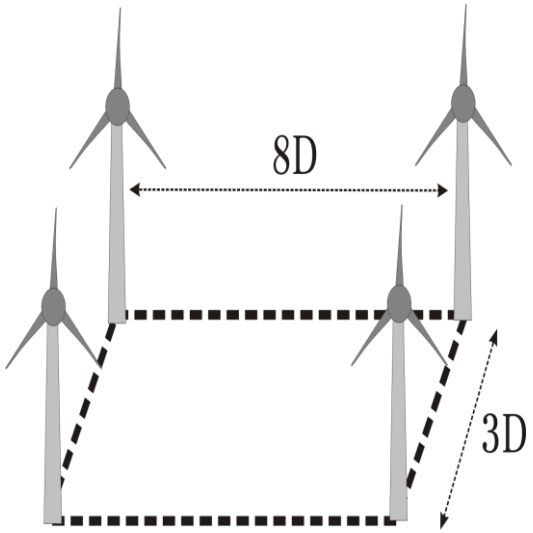

Figure 2 Scheme of the conventional marine wind farm layout

Provided the type of existing wind turbine is not changed, since we operate with lift-force type, and the wind conditions remain constant, the power density, σ_P, remains constant. A way to increase the power density, assuming permanent wind conditions, is the power coefficient improvement, which means changing the structure or elements of the lift-force wind turbine.

Journal of Offshore Structure and Technology
Research paper
Vol 11, issue 1,2024
Receiving date:18-5-2024
Acceptance- 21-05-2024
Publication 22-05-2024

Because we cannot change the lift-force wind turbine technology once installed, the only solution to increase the power density is the insertion of new wind turbines in the spot area (Figure 3).

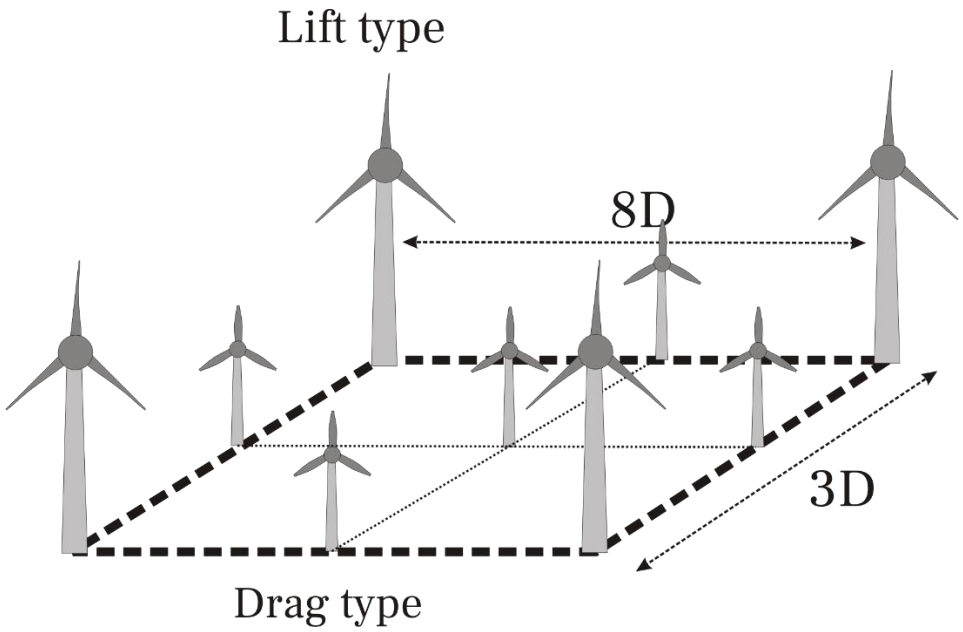

Figure 3. Scheme of the proposed marine wind farm layout

Drag-force wind turbines may be inserted because they use turbulent wind flow with high efficiency; besides, previous studies proved that the use of turbulent flow reduces the turbulence index leeward, thus limiting or avoiding the effects of the turbulent flow on the next wind turbine of the lift-force type [32].

According to set up characteristics for the wind turbines, 120 m diameter for the lift-force type, and keeping the distance ratio between adjacent lift-force turbines, 8D for leeward and 3D for side turbines, a single cell wind marine farm like the one drawn in Figure 2 of 960 m length and 360 m width.

Now, inserting a wind turbine of the drag-force type, with a 47.1 m diameter, the minimum distance between lift-force and drag-force wind turbines should be:

$$\begin{aligned} d_f &= 8x47.1 = 376.8\,m \\ d_s &= 3x47.1 = 141.3\,m \end{aligned} \qquad (13)$$

Journal of Offshore Structure and Technology
Research paper
Vol 11, issue 1,2024
Receiving date:18-5-2024
Acceptance- 21-05-2024
Publication 22-05-2024

These values impose a distance between two adjacent lift-force turbines of 753.6 m in the wind direction and 282.6 m sideways, 21% lower than the wind marine farm cell, thus fulfilling the distance ratio restriction.

Wake effects generate a reduction of performance on conventional horizontal wind turbines because of the vortex created by the turbulent flow that reduces the amount of available wind energy to be converted in rotational movement. In this situation, the behavior of a classical wind turbine is of lower performance since the ratio of lift-force to drag forces diminishes. The reduction of the lift-force provokes a lower torque, thus a reduction in the rotation speed and the power generation. Besides, the increase in the drag-forcecauses increased wear and decreases the efficiency of the wind turbine.

Drag-force wind turbines are currently of less power than the lift-force type ones; they operate at lower power efficiency; therefore, assuming a power coefficient of $C_P{}'$, for the drag-force type wind turbine and an output power of P', corresponding to a diameter of the wind turbine rotor, D', according to the new wind farm layout shown in Figure 3, it results:

$$\sigma_P^{'} = \frac{P+P^{'}}{S} = 4\frac{(1/2)C_p\rho(\pi/4)D^2u^3}{24D^2} + 5\frac{(1/2)C_p^{'}\rho(\pi/4)\left(D^{'}\right)^2u^3}{24D^2} = \frac{\pi}{48}C_p\rho u^3 + \frac{5\pi}{96}\left(\frac{D^{'}}{D}\right)^2 C_p^{'}\rho u^3 \tag{14}$$

If we define the power coefficient and diameter of the rotor of the drag-force wind turbine type in terms of the power coefficient and rotor diameter of the lift-force wind turbine type, we have:

$$\sigma_P^{'} = \frac{\pi}{48}C_p\rho u^3 + \frac{5\pi}{96}f_D^2 f_{C_P}C_p\rho u^3 = \frac{\pi}{96}C_p\rho u^3\left(2+5f_D^2 f_{C_P}\right) \tag{15}$$

Where:

$$f_D = \frac{D^{'}}{D};\ f_{C_P} = \frac{C_p^{'}}{C_p} \tag{16}$$

Combining equations 12 and 15, we obtain the ratio of the new to conventional layout power density of the marine wind farm:

$$\frac{\sigma_P^{'}}{\sigma_P} = 1 + 2.5 f_D^2 f_{C_P} \tag{17}$$

Analyzing equation 17, we notice that the increase in the output power depends on the size of the drag-force wind turbine and its efficiency.

Figure 4 shows the simulation of the power density ratio for different values of the factors of power coefficient and wind turbine rotor diameter.

Journal of Offshore Structure and Technology
Research paper
Vol 11, issue 1,2024
Receiving date:18-5-2024
Acceptance- 21-05-2024
Publication 22-05-2024

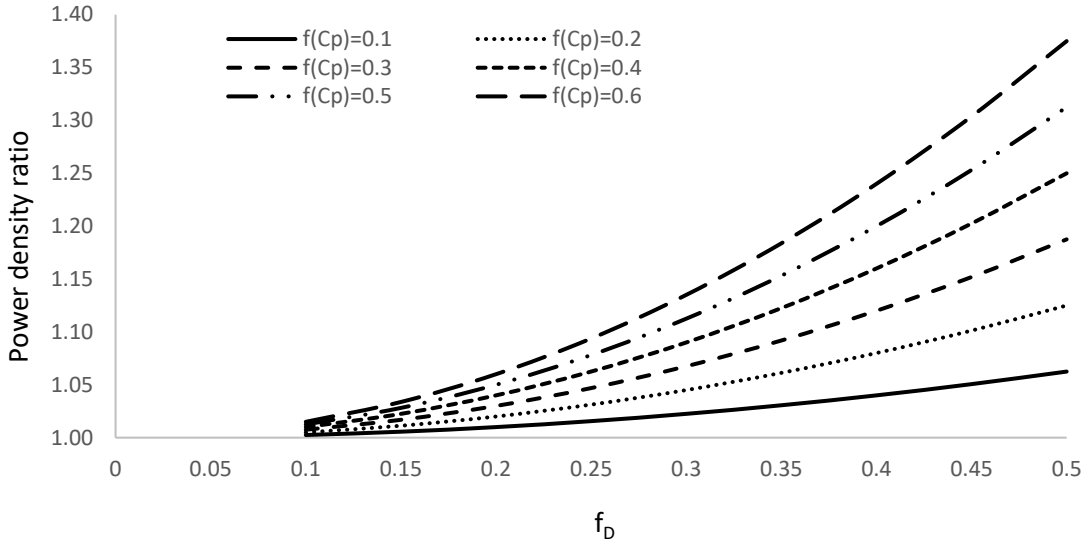

Figure 4 Ratio of the power density of the hybrid versus conventional offshore wind farm design as a function of the power coefficient factor and the diameter factor of the drag-force-type wind turbine versus the lift-force-type wind turbine

We observe that global output power increase rises to 37.5% for a high-quality drag-forcewind turbine with a power coefficient of around 0.24, which can be considered good enough and half the size of the giant wind turbines of the lift-force type.

Being conservative, considering a relatively moderate size and regular performance, we can operate with a power coefficient factor of 0.5 and a diameter factor of 0.4; these values correspond to a power coefficient of 0.20, assuming the lift-force type wind turbine operates at 40% of efficiency, and a size of 28 m of diameter for the wind turbine rotor. Operating with these values that can be considered standard for a drag-force wind turbine, the global output power gain is 20%, which means a considerable increase.

POWER GENERATION

Considering the simulated marine wind farm cell, the global output power is 32 MW for the conventional layout (Figure 2) and 38 MW for the new configuration (Figure 3); this represents a power increase of 15.8%.

Now, determining the f_D value for our configuration, which is $f_D = \frac{47.1}{120} = 0.393$ (18), applying this value to Figure 4, we observe that, for a power density ratio of 1.158, corresponding to an output power gain of 15.8%, the two values cross at $f(C_p)$=0.4, which matches with the setup value for the power coefficient for the wind turbines within 99.9% accuracy.

Journal of Offshore Structure and Technology
Research paper
Vol 11, issue 1,2024
Receiving date:18-5-2024
Acceptance- 21-05-2024
Publication 22-05-2024

The analysis of the output power shows a perfect matching between the wind farm cell layout and theoretical approach, which validates the developed analysis and proves the feasibility of the proposed configuration. The marine wind farm cell drawn in Figure 2 can be replicated the times the available area allows.

The 15.8 % output power gain with the proposed configuration may increase to 37.5%, as obtained in the theoretical analysis. If we consider a marine wind farm of 62 turbines of 8 MW each, like the one built in Saint Brieuc Bay (North of France) [33], we have 15 cells according to the wind turbine distribution (Figure 3) and Table 1.

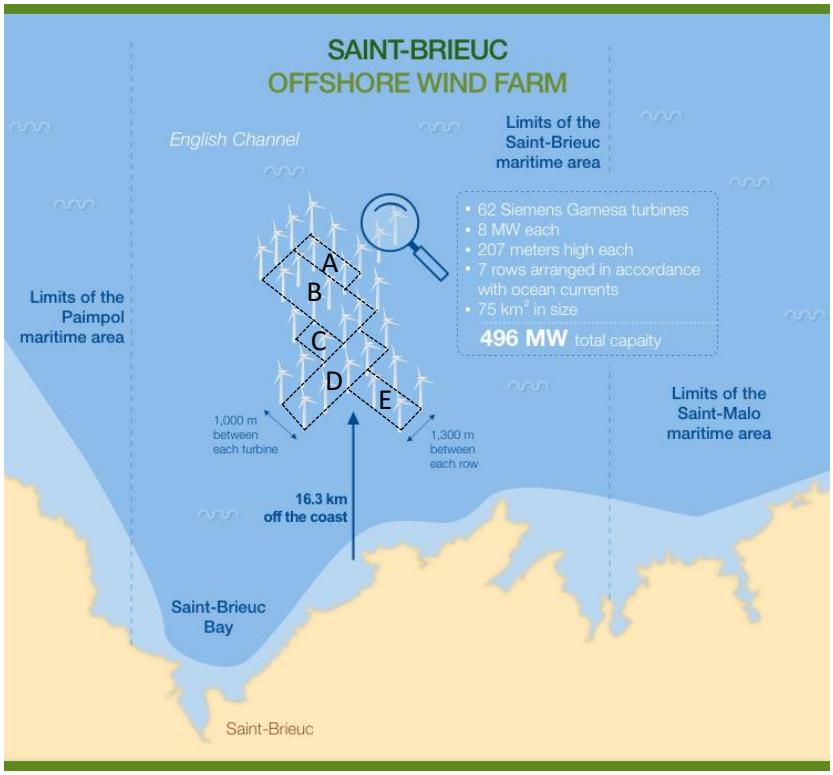

Figure 5 Layout of the marine wind farm at Saint Brieuc (France), including the simulated cell area for drag-force wind turbine installation

Table 1 Cell distribution for the marine wind farm at Saint Brieuc (France)

Zone	A	B	C	D	E
Cell number	2	6	1	4	2

Since every cell contains five drag-force wind turbines (Figure 3), the total number of inserted turbines is 75, representing a global output power of 90 MW; therefore, the wind farm power generation increases to 586 MW, 18.1% more than the conventional layout.

CONCLUSIONS

Journal of Offshore Structure and Technology
Research paper
Vol 11, issue 1,2024
Receiving date:18-5-2024
Acceptance- 21-05-2024
Publication 22-05-2024

The layout of a marine wind farm that operates with wind turbines of the lift-force type has been reconfigured, inserting drag-force wind turbines in the free space between the existing wind turbines. The drag-force wind turbines will be placed at the intermediate point between two adjacent wind turbines, either lengthwise or crosswise.

The increase in the global output power is due not only to the higher number of wind turbines of the lift-force type but also to the power generation due to the inserted drag-force wind turbines themselves.

The power gain depends on the size and quality of the inserted drag-force wind turbine, but it can reach up to 37.5% for optimum conditions and 20% for standard characteristics.

We obtain a 18% power generation increase in a commercial wind farm of 62 turbines of 8 MW output power if we implement the proposed configuration, intercalating drag-force wind turbines of 1.2 MW and 47.1 m diameter in the free space between the conventional wind turbines.

REFERENCES

[1] P. Hou, W. Hu, C. Chen, M. Soltani & Z. Chen, Optimization of offshore wind farm layout in restricted zones. Energy, Volume 113, pages 487 -496 (2016).

[2] P. Hou, W. Hu, M. Soltani & Z. Chen, Optimized placement of wind turbines in large-scale offshore wind farm using particle swarm optimization algorithm. IEEE Transactions on Sustainable Energy, Volume 6, Issue 4, pages 1272-1282m (2015).

[3] D. Ahn, S. C. Shin, S. Y. Kim, H. Kharoufi & H. C. Kim, Comparative evaluation of different offshore wind turbine installation vessels for Korean west–south wind farm. International Journal of Naval Architecture and Ocean Engineering, Volume 9, Issue 1, pages 45-54 (2017).

[4] Renewables First. The Hydro and Wind Company. How much wind turbine power could I generate from a wind turbine?. How much wind turbine power can I create - Renewables First. Accessed online: 23/11/2022

[5] Christiansen, M. B., & Hasager, C. B. (2005). Wake effects of large offshore wind farms identified from satellite SAR. Remote Sensing of Environment, 98(2-3), 251-268.

[6] Neumann, T. H. O. M. A. S., & Emeis, S. T. E. F. A. N. (2020). Long-range modifications of the wind field by offshore wind parks–results of the project WIPAFF. Meteorol. Z, 29, 355-376.

[7] X. Sun, D. Huang & G. Wu, The current state of offshore wind energy technology development. Energy, Volume 41, Issue 1, pages 298-312 (2012).

[8] W. Zhixin, J. Chuanwen, A. Qian & W. Chengmin, The key technology of offshore wind farm and its new development in China. Renewable and Sustainable energy reviews, Volume 13, Issue 1, pages 216-222 (2009).

Journal of Offshore Structure and Technology
Research paper
Vol 11, issue 1,2024
Receiving date:18-5-2024
Acceptance- 21-05-2024
Publication 22-05-2024

[9] J. K. Kaldellis, & M. Kapsali, Shifting towards offshore wind energy—Recent activity and future development. Energy policy, Volume 53, pages 136-148 (2013).

[10] Y. Guo, H. Wang & J. Lian, Review of integrated installation technologies for offshore wind turbines: Current progress and future development trends. Energy Conversion and Management, Volume 255, 115319 (2022).

[11] S. M. Muyeen, (Ed.). Wind energy conversion systems: technology and trends. Springer Science & Business Media (2012).

[12] H. Díaz, & C. G. Soares, Review of the current status, technology and future trends of offshore wind farms. Ocean Engineering, Volume 209, 107381 (2020).

[13] P. Jamieson, Innovation in wind turbine design. John Wiley & Sons (2018).

[14] Tahani, M., Maeda, T., Babayan, N., Mehrnia, S., Shadmehri, M., Li, Q., ... & Masdari, M. (2017). Investigating the effect of geometrical parameters of an optimized wind turbine blade in turbulent flow. *Energy conversion and management*, *153*, 71-82.

[15] Jeong, J., Park, K., Jun, S., Song, K., & Lee, D. H. (2012). Design optimization of a wind turbine blade to reduce the fluctuating unsteady aerodynamic load in turbulent wind. *Journal of mechanical science and technology*, *26*, 827-838.

[16] Jackson, K. J., Zuteck, M. V., Van Dam, C. P., Standish, K. J., & Berry, D. (2005). Innovative design approaches for large wind turbine blades. *Wind Energy: An International Journal for Progress and Applications in Wind Power Conversion Technology*, *8*(2), 141-171.

[17] Rashidi, M., Kadambi, J. R., & Ke, R. (2019, November). Wind energy harnessing system for low and high wind speeds. In *ASME International Mechanical Engineering Congress and Exposition* (Vol. 59445, p. V007T08A012). American Society of Mechanical Engineers.

[18] Chamorro, L. P., Tobin, N., Arndt, R. E. A., & Sotiropoulos, F. (2014). Variable-sized wind turbines are a possibility for wind farm optimization. *Wind Energy*, *17*(10), 1483-1494.

[19] A. N. Sanderasagran, A. B. Abd Aziz, A. N. Oumer & I. M. Sahat, Alternative Method of Nature Inspired Geometrical Design Strategy for Drag Induced Wind Turbine Blade Morphology. International Journal of Automotive and Mechanical Engineering, Volume 19, Issue 2, pages 9759-9772 (2022).

[20] M. R. Castelli, & E. Benini, Comparison between lift-force and drag-driven VAWT concepts on low-wind site AEO. World Academy of Science, Engineering and Technology, pages 1677-1682 (2011)

[21] Serrano, J. M., Domínguez-Navarro, J. A., Sevil, J. A., & López, R. D. (2018). A case study of floating offshore wind park in the Mediterranean. In International Conference on Renewable Energies and Power Quality (ICREPQ'18), Salamanca (Spain).

[22] Manwell, J. F., McGowan, J. G., & Rogers, A. L. (2010). Wind energy explained: theory, design and application. John Wiley & Sons.

Journal of Offshore Structure and Technology
Research paper
Vol 11, issue 1,2024
Receiving date:18-5-2024
Acceptance- 21-05-2024
Publication 22-05-2024

[23] Burton, T., Jenkins, N., Sharpe, D., & Bossanyi, E. (2011). Wind energy handbook. John Wiley & Sons.

[24] Bagchi, P., & Balachandar, S. (2003). Effect of turbulence on the drag and lift-force of a particle. Physics of fluids, 15(11), 3496-3513.

[25] Aghaei-Jouybari, M., Seo, J. H., Yuan, J., Mittal, R., & Meneveau, C. (2022). Contributions to pressure drag in rough-wall turbulent flows: insights from force partitioning. Physical Review Fluids, 7(8), 084602.

[26] Stoll, D., Schoenleber, C., Wittmeier, F., Kuthada, T., & Wiedemann, J. (2016). Investigation of aerodynamic drag in turbulent flow conditions. SAE International Journal of Passenger Cars-Mechanical Systems, 9(2016-01-1605), 733-742.

[27] Greaves, P. (2013). Fatigue analysis and testing of wind turbine blades (Doctoral dissertation, Durham University).

[28] Thomsen, K., & Sørensen, P. (1999). Fatigue loads for wind turbines operating in wakes. Journal of wind engineering and industrial aerodynamics, 80(1-2), 121-136.

[29] Armenta-Déu, C., Piqueras, D. (2024) Performance of Drag Offshore Floating Wind Turbine with variable pitch. Journal of Offshore Structure and Technology (publication pending)

[30] Armenta-Déu, C. (2024) Analysis of turbulent regime for fluid flow. Internal Report. Project IM-01-24

[31] Master in Energy. Chapter 3: Aerodynamics. Complutense University of Madrid 2023-24

[32] Fernández, R. (2024) Harnessing turbulent flow in marine wind parks: output power improvement. Master Thesis. Master in Energy. Faculty of Physics. Complutense University of Madrid.

[33] Saint-Brieuc offshore wind farm. Saint-Brieuc: Iberdrola's first large-scale offshore wind power project in Brittany. Iberdrola. https://www.iberdrola.com/about-us/what-we-do/offshore-wind-energy/saint-brieuc-offshore-wind-farm [Accessed online: 18/05/2024]